J. Fluid Mech. (1965), *vol.* 21, *part* 4, *pp.* 737–760
Printed in Great Britain

The steady separated flow past a circular cylinder at large Reynolds numbers

By ANDREAS ACRIVOS AND D. D. SNOWDEN
Department of Chemical Engineering, Stanford University
AND A. S. GROVE† AND E. E. PETERSEN
Department of Chemical Engineering, University of California, Berkeley

(Received 25 August 1964)

This paper is concerned with deducing the most important features of the steady separated flow past a circular cylinder in the limit of vanishing viscosity. First of all, it is shown that the experimental results reported in an earlier article cannot be reconciled with the notion that, as the Reynolds number Re is increased, the flow becomes inviscid everywhere and that viscous effects remain confined within infinitesimally thin shear layers. In contrast, the limiting solution is visualized as exhibiting three essential features: a viscous, closed 'wake bubble' of finite width but with a length increasing linearly with Re in which inertial and viscous effects are everywhere of equal order of magnitude; an outer inviscid flow; and, separating the two regions, a diffuse viscous layer covering large sections of the external field. Further properties of this asymptotic solution include: a finite form drag, a negative rear pressure coefficient at the rear stagnation point of the cylinder, and a Nusselt number for heat transfer which becomes independent of Re along the non-wetted portion of the cylinder surface. This model is shown to be consistent with all the experimental data presently available, including some new heat transfer results that are presented in this paper.

An approximate technique is also proposed which takes into account the asymptotic character of the flow in the vicinity of the cylinder and which predicts the pressure distribution around the cylinder in good agreement with the experiments.

1. Introduction

One of the basic unsolved problems of viscous flow theory is that of understanding the nature of the steady separated flow past bluff objects at high Reynolds numbers and of determining the limiting solution of the steady-state Navier–Stokes equations for vanishing viscosity. This is an important problem because, if this limiting solution were available, it could yield the pressure distribution around the object, thereby enabling one to calculate the rates of transport of vorticity, heat and mass for steady flows with finite (but small) viscosity with a standard boundary-layer analysis. Also, the successful solution of this problem would yield valuable information concerning the extent to which viscosity determines the structure of steady high-Reynolds-number flows.

† Present address: Fairchild Semiconductor Research Laboratory, Palo Alto, California.

To obtain the limiting solution theoretically is an extremely difficult task. As was already explained in an earlier article (Grove *et al.* 1964), all previous attempts seem to have been based on the simplifying assumption that the limiting solution of the Navier–Stokes equations for vanishing viscosity can be obtained by solving the simple limit of these equations, i.e. the Euler or inviscid equations. This assumption cannot be justified rigorously. Yet, it appears reasonable to suppose that, as the Reynolds number is increased, the viscous contributions to the Navier–Stokes equations should become negligible in comparison to inertial and pressure effects everywhere, except within thin regions where the velocity gradients become infinitely large. According to this point of view then, the flow field, with the exception of these singular surfaces, should be describable in terms of an inviscid solution provided that the viscosity is made sufficiently small.

During the past sixty years, such an approach has been applied with tremendous success to the solution of a great variety of problems associated with flows past slender bodies. In contrast, its application to flows past bluff objects, where separation takes place, has resulted in almost complete failure. To quote Proudman (1960): '...it is a sobering thought that, despite the fifty or so years that the techniques of boundary-layer theory have been at our disposal, so little progress has been made with the problem (of separated flows) that even such a bulk characterististic as the dependence of the drag coefficient on (large) Reynolds number is still a matter of pure conjecture.'

Offhand, one might think that the basic difference between the two cases is the following. When separation does not take place, velocity discontinuities will occur only at the body surface, and the Euler equations will have a unique solution. If, however, separation does take place, there will be additional surfaces of velocity discontinuity whose shape and position are unknown. Consequently, the Euler equations will have an infinite number of solutions, such as the symmetrical potential flow model, the Kirchhoff free-streamline solution, the proposal of Batchelor (1956) and Föppl's vortex model (Grove *et al.* 1964), and it is impossible to tell *a priori* which one of the inviscid solutions, if any, will correctly describe the asymptotic nature of the steady flow at high Reynolds numbers.†

In order then to provide a much needed physical basis for a theoretical attack on this problem, an experimental investigation of the steady separated flow past a circular cylinder at increasingly large Reynolds numbers was undertaken, the principal features of which have already been described in detail by Grove *et al.* (1964). It is worthwhile to recall here the most important results of these experiments. (i) The pressure coefficient (or non-dimensional pressure)‡ at the

† Actually, as was pointed out to the authors by Dr G. K. Batchelor, Föppl's model cannot be classified as being an acceptable solution of the Navier–Stokes equations for arbitrarily small but non-vanishing viscosity, owing to the fact that the vorticity which is assumed to be concentrated at the two vortex centres cannot be prevented from diffusing out into the main part of the closed wake, unless of course $\nu \equiv 0$.

‡ The pressure coefficient is defined as $p_\theta = (p'_\theta - p'_{\text{stat}})/\frac{1}{2}\rho U^2$ where p'_θ is the actual pressure at the cylinder surface at an angle θ from the front stagnation point, ρ is the fluid density, and p'_{stat} and U are, respectively, the static pressure and velocity of the undisturbed flow. Primed symbols in this paper usually refer to physical, dimensional quantities.

rear stagnation point of the cylinder, p_{180}, reaches the value of approximately $-0{\cdot}45$ at Re $= 25$ and remains unchanged as the Reynolds number is increased.† (ii) Within the range of the experiments, the length of the circulating wake bubble is proportional to the Reynolds number, while, in contrast, the width of the wake-bubble reaches a finite limit which is only slightly larger than the cylinder diameter. (iii) The ratio of the maximum back-flow velocity within the wake bubble to the velocity of the undisturbed flow reaches a finite limit which lies approximately between $-0{\cdot}3$ and $-0{\cdot}5$.

It is now the purpose of this paper to draw some conclusions regarding the nature of steady separated flows at large Reynolds numbers based chiefly on the new experimental results given by Grove *et al.* (1964) and briefly summarized above.

2. A theoretical model for the limiting solution

(*a*) *The flow structure inside the wake bubble*

We begin our theoretical analysis by focusing our attention on the experimental results pertaining to the pressure coefficient at the rear stagnation point of the cylinder. These measurements have already been presented in figure 6 of Grove *et al.* (1964) but, because of their significance, they are reproduced in figure 1 together with a few recent data. In contrast with figure 6 of Grove *et al.*, all the points shown in figure 1 refer to steady wakes.

This graph can now be interpreted in two ways. One could take the point of view of course that, since the maximum Reynolds number Re attained experimentally was only about 180, it is not possible to infer from figure 1 the asymptotic limit of the rear pressure coefficient as $\mathrm{Re}\to\infty$, and that the plateau of the curve of pressure coefficient against Re in the range $25 < \mathrm{Re} < 180$ may be caused by some sort of transitory flow régime. A much more constructive attitude, however, would be to assume that the rear pressure coefficient would remain equal to $-0{\cdot}45$ even for Re > 180, and to construct a theoretical model for the steady flow at infinite Re which would be consistent with this experimental result. This approach seems all the more logical, since a careful examination of all the experimental data presented in figure 1 shows that, within the experimental accuracy, the rear pressure coefficient is clearly independent of Re for

$$25 < \mathrm{Re} < 180,$$

and that no systematic trend can be discerned among the various points away from the horizontal line.

We shall take it for granted then that the asymptotic solution must be characterized by a rear pressure coefficient equal to $-0{\cdot}45$. This, as we shall show presently, leads to a number of significant conclusions.

The first important result is that the pressure drag for the cylinder must remain finite even for infinite Reynolds numbers. This is based on the fact that the pressure coefficient at the front stagnation point must obviously be equal to unity for large Re, and that, as stated by Grove *et al.*, the pressure coefficient is

† The Reynolds number is $\mathrm{Re} = Ud/\nu$, where U is the velocity of the undisturbed stream, d is the cylinder diameter and ν is the kinematic viscosity.

approximately equal to p_{180} throughout the rear or 'non-wetted' part of the perimeter. Thus, since p_{180} equals $-0{\cdot}45$ at high Re, only an extremely unrealistic pressure profile on the front half of the cylinder, a profile that would depart widely from those measured experimentally, could produce a zero pressure drag (Grove 1963).

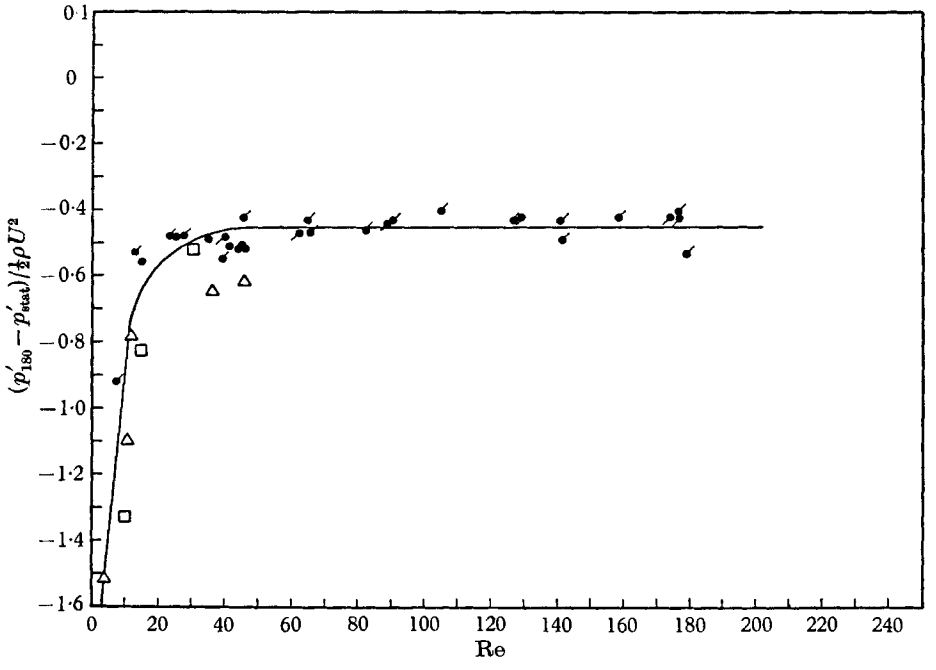

FIGURE 1. The effect of Reynolds number on the rear stagnation pressure (steady wake). ●, no splitter plate; ◐, 4 in. splitter plate; ◑, 2 in. splitter plate; □, Homann; △, Thom.

An immediate consequence of the finite drag conclusion is of course that the asymptotic flow at high Reynolds numbers cannot consist of a truly finite wake with its dimensions independent of Re, since, under these conditions, a zero pressure drag would result in accordance with d'Alembert's principle.

The wake bubble must then continue to grow, but, since its width was experimentally found to become independent of Re (see Grove *et al.*), we need only concern ourselves with the increase in its length. Let us consider the typical wake bubble depicted in figure 2. We observe first of all that a closed streamline which passes near the non-wetted side of the cylinder must also pass through a region lying close to the wake stagnation point. There, however, the pressure coefficient is most certainly either close to zero, or even positive on account of the relatively stagnant nature of the flow, whereas, as mentioned earlier, the pressure coefficient along the cylinder surface is equal to $-0{\cdot}45$. One is forced to admit, therefore, that, along any given streamline connecting the rear portion of the wake bubble with the region close to the cylinder, there must exist a significant pressure drop which remains finite for all Re. Clearly, this pressure drop can be due only to viscous effects.

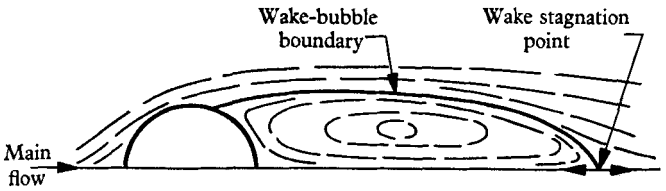

FIGURE 2. A typical wake bubble.

Thus, we have reached the seemingly paradoxical conclusion that, even when $\mathrm{Re} \to \infty$, the flow inside the wake bubble cannot be treated as inviscid and that viscous effects must be retained in order to account for the observed pressure drop. This result will now be given a surprisingly simple explanation.

We recall that, in terms of non-dimensional variables, the Navier–Stokes equations for the two-dimensional steady case are

$$u\frac{\partial u}{\partial x}+v\frac{\partial u}{\partial y}=-\frac{1}{2}\frac{\partial p}{\partial x}+\frac{1}{\mathrm{Re}}\nabla^2 u, \tag{1a}$$

and

$$u\frac{\partial v}{\partial x}+v\frac{\partial v}{\partial y}=-\frac{1}{2}\frac{\partial p}{\partial y}+\frac{1}{\mathrm{Re}}\nabla^2 v, \tag{1b}$$

to which must be added the continuity equation

$$\frac{\partial u}{\partial x}+\frac{\partial v}{\partial y}=0. \tag{2}$$

(The velocities have been reduced by U, the distances by the cylinder diameter d, the pressure as before, and $\mathrm{Re} = Ud/\nu$. The undisturbed flow is in the positive x-direction.)

Now, it has already been reported by Grove *et al.* that, along the major portion of the returning stagnation streamline, the flow velocity is $O(1)$ and that the width of the wake bubble is also $O(1)$ and independent of the Reynolds number. Consequently, if in the above system of equations the viscous and the inertia terms are to remain of the same order of magnitude even as $\mathrm{Re} \to \infty$, we must require that both $\partial p/\partial x$ and $\partial u/\partial x$ be $O(1/\mathrm{Re})$. This in turn suggests the substitution

$$\hat{x}=\frac{x}{\mathrm{Re}}, \tag{3}$$

in terms of which the equations of motion become, as $\mathrm{Re} \to \infty$,

$$u\frac{\partial u}{\partial \hat{x}}+\hat{v}\frac{\partial u}{\partial y}=-\frac{1}{2}\frac{\partial p}{\partial \hat{x}}+\frac{\partial^2 u}{\partial y^2}, \tag{4a}$$

and

$$\frac{\partial p}{\partial y}=0, \tag{4b}$$

where

$$\hat{v}=-\int_0^y \frac{\partial u}{\partial \hat{x}}\,dy. \tag{5}$$

An immediate consequence of this analysis is that the wake-bubble length x_L should be a linear function of Re and that the shape of the wake bubble in the

$(\hat{x}, y)$-plane should be independent of the Reynolds number. Both these theoretical predictions are in agreement with the experimental observations reported by Grove *et al.*

It is also of some interest to point out that, since the return (negative) velocity has its maximum value along the returning streamline, $(\partial^2 u/\partial y^2)_{y=0} > 0$ for $0 < \hat{x} < \hat{x}_L$, where $\hat{x} = 0$ denotes the rear stagnation point of the cylinder and $\hat{x}_L$ the position of the wake stagnation point. Therefore, by integrating equation (4*a*) along $y = 0$, we arrive at

$$p(\hat{x}_L) - p_{180} = 2\int_0^{\hat{x}_L} \left(\frac{\partial^2 u}{\partial y^2}\right)_{y=0} d\hat{x} > 0, \tag{6}$$

which is, once more, in qualitative agreement with the experimental measurements.

(*b*) *The state of motion near the non-wetted perimeter of the cylinder*

Although equations (4) and (5) may very well describe the state of motion throughout the major portion of the wake bubble, it becomes apparent upon further examination that they cannot hold near the cylinder surface. The reason for this can be traced to the omission of the term $\partial^2 u/\partial \hat{x}^2$ from (4*a*) and the resulting reduction of the order of that equation. Consequently, if one were to attempt a solution of this system in the $(\hat{x}, y)$-plane (in which, incidentally, the cylinder appears as a vertical flat plate when $\mathrm{Re} \to \infty$) one would be forced to abandon one of the boundary conditions, $\hat{v} = 0$ at $\hat{x} = 0$, and require only that $u = 0$ at $\hat{x} = 0$. It is clear then that, for the region near the cylinder, a new transformation is needed which would eliminate once again the Reynolds number from equations (1) and (2) without, however, reducing their order.

Such a transformation is given by

$$\bar{u} = u\mathrm{Re}, \quad \bar{v} = v\mathrm{Re} \quad \text{and} \quad \bar{p} = p\mathrm{Re}^2, \tag{7}$$

in terms of which equations (1) and (2) become, respectively,

$$\left.\begin{aligned} \bar{u}\frac{\partial \bar{u}}{\partial x} + \bar{v}\frac{\partial \bar{u}}{\partial y} &= -\frac{1}{2}\frac{\partial \bar{p}}{\partial x} + \nabla^2 \bar{u}, \\ \bar{u}\frac{\partial \bar{v}}{\partial x} + \bar{v}\frac{\partial \bar{v}}{\partial y} &= -\frac{1}{2}\frac{\partial \bar{p}}{\partial y} + \nabla^2 \bar{v}, \\ \text{and} \qquad \frac{\partial \bar{u}}{\partial x} + \frac{\partial \bar{v}}{\partial y} &= 0. \end{aligned}\right\} \tag{8}$$

Of course, before concluding that $\bar{u}$ and $\bar{v}$ are independent of Re and are functions of position alone, we must be able to show that the Reynolds number, which has been eliminated from equations (1), does not enter into the solution via the boundary conditions. These boundary conditions must therefore be examined in some detail.

First of all, we require that $\bar{u}$ and $\bar{v}$ vanish along the non-wetted portion of the cylinder surface and that, because of symmetry, $\partial \bar{u}/\partial y$ and $\bar{v}$ be zero along the stagnation streamline. In addition, we require that, in accordance with the usual procedure for singular perturbation expansions, the 'inner' solution $\bar{u}(x, y)$

match throughout an overlap region with the 'outer' solution $u(\hat{x}, y)$ satisfying equations (4) and (5). This matching requirement becomes

$$\lim_{x\to\infty} \overline{u}(x, y) = \lim_{\hat{x}\to 0} \operatorname{Re} u(\hat{x}, y), \tag{9}$$

if the Reynolds number Re is allowed to take on arbitrarily large values. Let us consider the right-hand side of equation (9). We have remarked already that if one sets $u = 0$ at $\hat{x} = 0$ one is not at liberty to specify, simultaneously, $\hat{v}(0, y)$. In general then the latter will be $O(1)$ and therefore, from the continuity equation, $(\partial u/\partial \hat{x})$ will also be $O(1)$ as $\hat{x} \to 0$. Thus,

$$u \to \hat{x} f(y) \quad \text{as} \quad \hat{x} \to 0,$$

where $f(y)$ is a function of y only, and, in view of equation (9)

$$\overline{u} \to x f(y) \quad \text{as} \quad x \to \infty.$$

Now, all the boundary conditions on $\overline{u}$ and $\overline{v}$, shown above, have clearly been independent of the Reynolds number. The remaining condition, however, which requires that $\overline{u}$ and $\overline{v}$ match along the region adjacent to the wake-bubble boundary with the appropriate velocity components of the external flow, cannot be given a simple form, owing to obvious analytical difficulties and to the complicated nature of the boundary-layer separating the main flow from the relatively stagnant 'inner' region of the wake bubble. Thus, we have not been able to determine whether or not the Reynolds number enters explicitly into this last matching condition. Nevertheless, although our theoretical arguments are admittedly incomplete, it seems reasonable to conclude tentatively that $\overline{u}$ and $\overline{v}$ are indeed independent of Re, and therefore $O(1)$ throughout the 'inner' region. As a consequence, the actual velocity components u and v should be $O(1/\mathrm{Re})$ within that portion of the wake bubble extending a distance $O(1)$ downstream from the non-wetted perimeter.

It was thought desirable to put this interesting conclusion to an experimental test. This was accomplished by means of a heat-transfer experiment, which was based on the following considerations. One recalls that, in forced convection, the temperature distribution around a heated object is governed by the energy equation

$$u\frac{\partial T}{\partial x} + v\frac{\partial T}{\partial y} = \frac{1}{\mathrm{Re}\,\mathrm{Pr}}\nabla^2 T \quad \text{(in dimensionless form)}, \tag{10}$$

where T is a dimensionless temperature and $\mathrm{Pr} \equiv c_p \mu/k$ is the familiar Prandtl number. Now, it is a well known fact that the thermal region is generally confined close to the heated surface if the Prandtl number of the fluid is large enough, in which case the temperature profile near the non-wetted part of the cylinder surface should be governed by the velocity distribution within the 'inner' region of the wake bubble, where, according to our earlier arguments, both u and v should be $O(1/\mathrm{Re})$ when $\mathrm{Re} \gg 1$. Thus, if we set $\overline{u} = u\,\mathrm{Re}$ and $\overline{v} = v\,\mathrm{Re}$, where $\overline{u}$ and $\overline{v}$ are $O(1)$, we obtain in place of equation (10)

$$\overline{u}\frac{\partial T}{\partial x} + \overline{v}\frac{\partial T}{\partial y} = \frac{1}{\mathrm{Pr}}\nabla^2 T, \tag{10a}$$

according to which the temperature distribution in the 'inner' region of the wake bubble should be independent of Re at high Reynolds numbers. In particular, since the thickness of the thermal layer becomes $O(\mathrm{Pr}^{-\frac{1}{3}})$ and therefore vanishingly small as $\mathrm{Pr} \to \infty$, one can introduce into equation (10*a*) the standard thermal-boundary-layer approximations (Lighthill 1950; Morgan & Warner 1956), from which it follows that

$$\mathrm{Nu}/\mathrm{Pr}^{\frac{1}{3}} = F(\theta) \quad \text{as} \quad \mathrm{Re} \to \infty, \tag{11}$$

where Nu is the local Nusselt number and $F(\theta)$ is an arbitrary function of the polar angle θ.

Thus, this analysis has led to the surprising conclusion that, along the non-wetted part of the cylinder surface, the local Nusselt number should become independent of Re in the limit $\mathrm{Re} \to \infty$, which is in contrast to the result for the wetted portion of the perimeter, where $\mathrm{Nu}/\mathrm{Pr}^{\frac{1}{3}}$ should be $O(\mathrm{Re}^{\frac{1}{2}})$ in accordance with the well-known laminar boundary-layer theory.

The experiments which were performed to test this conclusion involved the measurement of the surface temperature distribution along a uniformly heated cylinder 0·82 in. in diameter, and were carried out in the oil tunnel already described by Grove *et al.* (The Prandtl number of the oil was in excess of 1000 thus ensuring the applicability of the thermal-boundary-layer approximation.) We shall now present very briefly the most important experimental findings, leaving the pertinent details of the experimental set-up to Appendix 1 at the end of this paper.

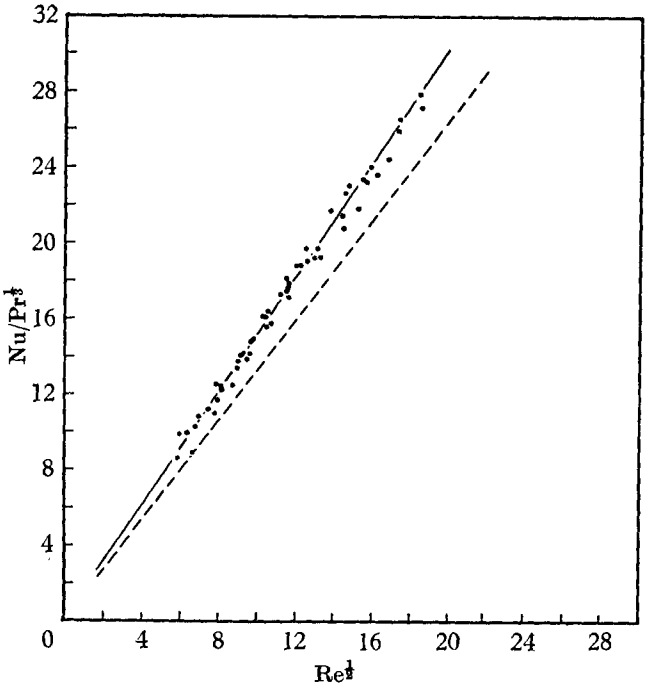

FIGURE 3. The effect of Reynolds number on $\mathrm{Nu}/\mathrm{Pr}^{\frac{1}{3}}$ at the front stagnation point. ●, Experimental; – – –, theoretical, $\mathrm{Nu}/\mathrm{Pr}^{\frac{1}{3}} = 1{\cdot}32\,\mathrm{Re}^{\frac{1}{2}}$.

In order to test the performance of the equipment, the experiments pertaining to the front stagnation point of the cylinder were first analysed, since these can be compared quantitatively with the predictions of the laminar-boundary-layer theory. These results are seen plotted in figure 3, from which it is apparent that $Nu/Pr^{\frac{1}{3}}$ becomes proportional to $Re^{\frac{1}{2}}$ for $Re > 40$. Although this asymptotic behaviour is of course in agreement with the theory, one observes a noticeable discrepancy in the proportionality constant between the theoretical value of 1·32, obtained from Lighthill's (1950) solution, and the experimental value of 1·50. The major part of this discrepancy is due undoubtedly to the presence of a wall effect, which, as shown by Grove *et al.*, is significant even for a blockage ratio as low as 0·1. This was further demonstrated with experiments using an even larger blockage ratio of 0·18, where the proportionality constant was found to equal 1·7.

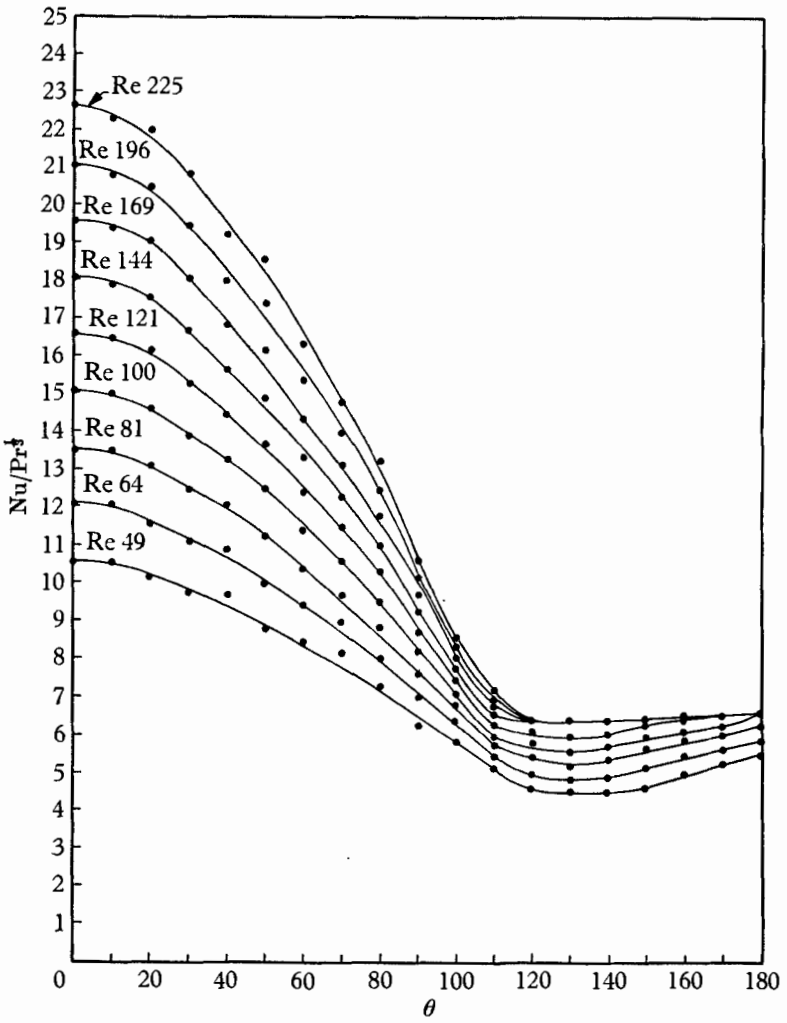

FIGURE 4. The variation of $Nu/Pr^{\frac{1}{3}}$ along the cylinder surface (steady wake).

Unfortunately, it was not found possible to repeat our heat-transfer experiments with a lower blockage ratio, owing to the great difficulties involved in fabricating a small diameter test piece with thin enough walls (i.e. less than 0·003 in. thick) to eliminate conduction losses along the perimeter. It should be kept in mind, therefore, that our experimental heat-transfer results, although qualitatively correct and thus adequate for the purposes of this study, do contain an error due to the wall effect of the order of 10–20 %.

Local values of $Nu/Pr^{\frac{1}{3}}$ are seen plotted in figure 4 for various values of θ and the Reynolds number. As expected, $Nu/Pr^{\frac{1}{3}}$ increases monotonically with Re along the wetted perimeter, becoming eventually proportional to $Re^{\frac{1}{2}}$, whereas, in accordance with the theoretical arguments presented above, it becomes gradually independent of Re along the non-wetted perimeter as the Reynolds number is increased. Another point of interest is that the local values of $Nu/Pr^{\frac{1}{3}}$ were found to be practically independent of position throughout the portion of the cylinder surface in contact with the wake bubble.

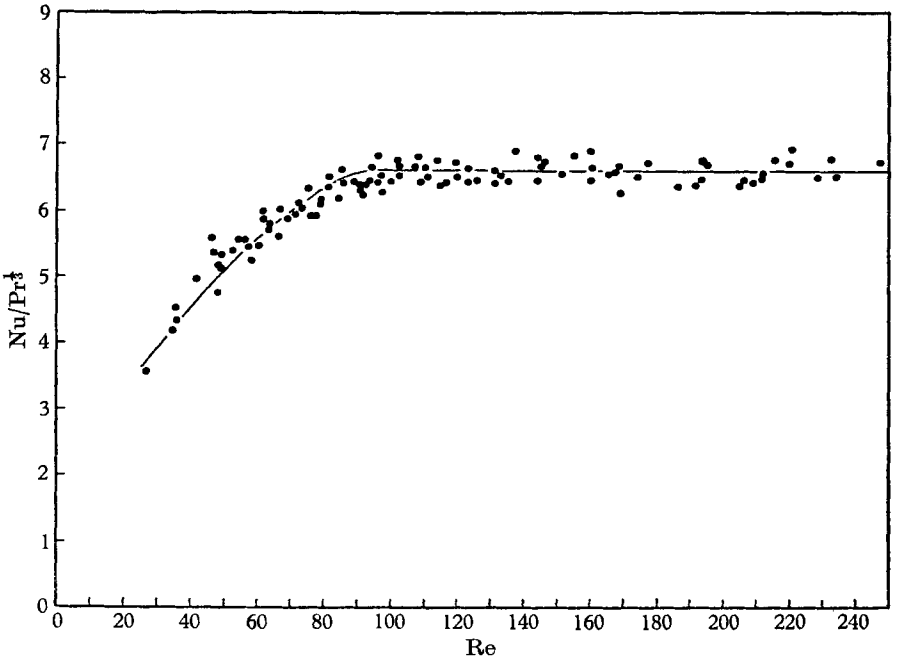

FIGURE 5. The effect of Reynolds number of $Nu/Pr^{\frac{1}{3}}$ at the rear stagnation point (steady wake).

Perhaps, though, the most important results are those depicted in figure 5 showing the variation with the Reynolds number of $Nu/Pr^{\frac{1}{3}}$ at the rear stagnation point. Indeed, the general behaviour of the experimental data is in striking agreement with the qualitative predictions of the theoretical analysis presented above, and clearly shows that, as long as the wake bubble remains steady, the local Nusselt number along the non-wetted perimeter approaches a finite limit as the Reynolds number is increased. That the transfer of heat in the wake bubble

must occur by convection, as our theory would demand, rather than by pure conduction which would also result in the Nusselt number being independent of Re, can be inferred from the magnitude of the experimentally measured Nu. Thus, as seen from figure 5, the asymptotic value of Nu is around 70, the Prandtl number being approximately 1200, which is about one or two orders of magnitude larger than the expected Nusselt number for pure conduction.

A graph very similar to figure 5 was also obtained with the 1·75 in. diameter heated cylinder, giving a blockage ratio of 0·18, the only difference being that the asymptotic value of $\mathrm{Nu}/\mathrm{Pr}^{\frac{1}{3}}$ was 13 rather than 6·5, and that the Reynolds number at which the asymptotic limit seemed to have been reached was 180 rather than 90. Thus it appears that, as was the case with the front part of the cylinder, the net affect of the proximity of the walls is to introduce an inaccuracy into the functional relation between Nu and Re along the non-wetted perimeter, without, however, affecting qualitatively its principal characteristic features.

Finally, it was thought desirable to repeat a few of these experiments, again with a blockage ratio of 0·08, but with the splitter plate absent. This arrangement gave an unsteady wake for $\mathrm{Re} > 65$ and produced results at the rear stagnation point which were quantitatively similar to those of figure 5. This is not too surprising, however, since it was observed during the experiments that the region close to the non-wetted perimeter appeared to remain quite steady, even when the major portion of the wake bubble was either unsteady or in a state of disintegration. Nevertheless, these two sets of results did differ in one important respect, since in every run involving unsteady wakes a definite upward trend in the curve of $\mathrm{Nu}/\mathrm{Pr}^{\frac{1}{3}}$ against Re was observed even along its flatter portions, whereas, in the case of steady wakes, such an upward trend was totally absent when $\mathrm{Re} > 90$.

It is realized, of course, that these heat-transfer results can only serve to test the consistency of the theoretical analysis presented so far, and that they cannot take the place of any direct experimental determination of the velocity components u and v within the 'inner' portion of the wake bubble. The data presented in figure 5 are valuable, however, since they provide further experimental evidence in support of our theoretical approach.

(*c*) *A possible inconsistency of the model*

Up to this point, we have focused our attention on the state of motion inside the wake bubble, and have developed a model for the flow there which is consistent with all the experimental measurements presently available. Yet, as pointed out to the authors by Dr G. K. Batchelor, a look at the flow outside the wake bubble gives rise to a serious question regarding the overall consistency of our theoretical treatment, which we shall now discuss.

A logical consequence of the arguments leading from equations (1) to equations (4) is that the pressure gradient along the major portion of the wake-bubble boundary should not be less than $O(1/\mathrm{Re})$, for otherwise, owing to the presence of viscous effects, it would not be possible to maintain a significant reverse flow within the wake bubble over longitudinal distances $O(\mathrm{Re})$. On the other hand,

a straightforward potential-flow analysis over the long but slender body representing the cylinder plus the wake bubble easily leads to the result that the pressure recovery should be almost complete at a distance $O(1)$ behind the cylinder, and that if, as we have claimed all along, the wake bubble has a width $O(1)$ but a length $O(\mathrm{Re})$, the pressure coefficient should be $O(1/\mathrm{Re})$ at a distance $O(1)$ downstream from the solid object. This in turn would mean that $\partial p/\partial x$ would be $O(1)$ along the 'inner' region of the wake bubble, i.e. the region lying within a distance $O(1)$ from the non-wetted perimeter, and at most $O(1/\mathrm{Re}^2)$ along the remaining portion of the closed wake. Both these results are in obvious contradiction with some of the basic aspects of our theoretical model.

An even more disturbing feature of this inviscid analysis, however, is that it leads to the conclusion that, since the pressure is supposed to recover a few diameters downstream from the cylinder, the pressure coefficient at the rear stagnation point cannot stay negative as $\mathrm{Re} \to \infty$ owing to the absence of any viscous effects along the returning streamline over distances $O(1)$. This, of course, is at variance with the experimental data shown in figure 1.

Thus, a truly inviscid analysis over the composite body, i.e. the cylinder plus the wake bubble, leads to conclusions that are hopelessly inconsistent not only with many of the basic features of our theoretical model, but, more important than that, with the experimental measurements pertaining to the pressure coefficient along the non-wetted perimeter of the cylinder.

To be sure, one may attempt to resolve the difficulty just described by arguing that the inconsistency may not be a real one after all, since it may merely arise out of the erroneous comparison of an inviscid analysis, which applies only at truly infinite Re, with experimental data that exist only up to $\mathrm{Re} \sim 200$. As mentioned earlier, however, considering all the evidence presently available, it appears much more reasonable to assume that the data, especially those in the range $100 < \mathrm{Re} < 200$, are indeed indicative of the state of motion at infinite Re, in which case one is faced with the task of showing why the classical potential flow treatment outlined above may not, in fact, be applicable to this particular system.

We recall at this point that the standard inviscid flow analysis has invariably been applied to objects which are fixed in size. For such systems, the analysis can be justified on the grounds that, at high Reynolds numbers $\mathrm{Re}_l = Ul/\nu$, the thickness of the viscous layers is everywhere, i.e. both adjacent to the body as well as throughout the wake, $O(l/\sqrt{\mathrm{Re}_l})$, thus becoming infinitesimally small as $\mathrm{Re} \to \infty$. The situation is altered in a very fundamental way, however, if, as in our case, the length of the object is allowed to vary in direct proportion to Re (based on the cylinder diameter), for, under these conditions, the thickness of the shear layer that separates the wake-bubble boundary from the external flow will become at least $O(1)$ near the tip of the wake bubble irrespective of the value of Re. Thus, the potential flow analysis should be performed, if at all, around an 'equivalent' body that would include not only the cylinder plus the wake bubble but also all the regions of non-zero vorticity. In view of the fact, however, that these shear regions cannot be made arbitrarily thin by increasing the Reynolds number, as would be the case with a body of fixed size, one has very little assur-

ance that the relative dimensions of the 'equivalent' body would be even qualitatively similar to those of the wake bubble. In particular, since the width of the outer (open) wake must increase parabolically with the longitudinal distance far downstream from the object, one has every reason for believing that the 'equivalent' body would be not only much longer (perhaps even open downstream) but also substantially wider than the composite body shown in figure 2.

The arguments presented above do not imply, of course, that the main features of the inviscid analysis over a slender body, resulting in the prediction of a pressure recovery within a distance $O(1)$ from the cylinder, are necessarily incorrect if applied to the present case. Instead, these arguments have focused attention on the very great complexity of the external flow problem, and have served to point out the tremendous difficulty involved in obtaining even qualitative deductions about the pressure distribution along the wake bubble on the basis of a truly inviscid model, owing to the fact that even the relative dimensions of the 'equivalent' body cannot be specified with confidence.

Thus, although we have not succeeded in resolving, once and for all, the possible inconsistency in our theoretical model, we have presented definite reasons why the inviscid flow analysis, which leads to this inconsistency, may in itself be incorrect. This matter is, however, far from settled yet and clearly requires considerably more attention.

3. Some approximate results

(*a*) *An approximate calculation of the pressure profile*

From a practical point of view, one of the most valuable results of any theoretical analysis of steady separated flows at high Re is the prediction of the pressure distribution around the solid object. Yet, this is also one of the most difficult problems to solve exactly since, as was explained in the last section, a truly inviscid analysis of the flow external to the cylinder and the wake bubble cannot be reconciled with the available experimental data. Thus, a more sophisticated approach appears necessary, an approach that would take into account the presence of non-zero vorticity throughout large portions of the external field. This, however, remains to be accomplished.

In the absence of an exact method, one is forced then to resort to approximate techniques, all of which, so far, have been based on an inviscid analysis of the flow system. At first glance, this may seem strange indeed in view of all that was said earlier on this subject. On the other hand, if it is well understood that the purpose of such an analysis is to yield approximate values for the pressure profile on the solid object, and very little else, then such a procedure is certainly permissible even though it may be incompatible with some of the main characteristic features of the flow. A case in point is the method first proposed by Roshko (1954), who performed an inviscid analysis for a composite body, consisting of the solid object together with a semi-infinite stagnant wake of finite width. In Roshko's analysis the (negative) wake pressure was left unspecified. Yet, even so, it was still not found possible to satisfy all the boundary conditions of the problem without introducing into the model a distinct inconsistency in the form of two semi-infinite solid plates parallel to the main

stream, the purpose of which was to force the stagnant wake to remain finite in width.

In regard to this problem, the use of such artifices is of course fairly standard by now, and the various additional models which have been proposed such as Riabouchinsky's (1920), Woods' (1955), Wu's (1962), to name but a few, differ mainly in the type of inconsistency which they introduce into an otherwise straightforward inviscid analysis. Of these models, Woods' (1955) and Roshko's (1954) (the latter refined by Wu 1962) appear to be the more successful ones, having given pressure profiles in good agreement with experimental measurements in the case of systems with *unsteady* wakes. When applied to steady separated flows, however, both these models are generally unsatisfactory, even when, as in Roshko's (1954) case, the wake pressure is set equal to that measured experimentally along the non-wetted perimeter of the object. It was thought desirable, therefore, to develop a new method for attacking this problem, which would yield a pressure distribution around a cylinder in agreement with the one measured experimentally at Re = 177 and shown in figure 4 of Grove *et al.* (1964).

The method which we shall propose consists simply of an inviscid analysis around a suitable composite body, as in figure 2, together with the assumption of zero pressure drop in the vertical direction throughout the wake bubble. The calculations can be performed most easily by means of Riegels' (1948) approximate technique,† according to which, if the body contour is expressed as $Y(X)$, where X is the axial distance from the front stagnation point of the cylinder (both distances being in terms of the cylinder radius)

$$u(X) = [1+\{Y'(X)\}^2]^{-\frac{1}{2}}\left[1+\frac{1}{\pi}P\int_0^L \frac{Y'(s)}{X-s}\,ds\right], \tag{12}$$

in which $u(X)$ denotes the tangential velocity along the body contour, L is the length of the body, the prime indicates differentiation and P the principal value of the integral. Then, because of Bernouilli's equation, the pressure distribution is

$$p(X) = 1-u^2(X),$$

where p is as defined earlier.

Clearly, there are two rather obvious requirements for the success of the proposed approach. First of all, since the function $Y(x)$ is assumed known in equation (12), one should be able to estimate *a priori* the general shape of the body contour. Fortunately, this can be accomplished without much difficulty in general due to the considerable information presently available concerning wake-bubble shapes. In addition, the calculated pressure profiles on the cylinder surface should not only agree with the experimental measurements, but should also be relatively insensitive to the shape of the assumed body contour.

As described in Appendix 2, a two parameter family of contours was chosen for detailed study. One of these contours is shown in figure 6 together with the experimentally observed wake-bubble boundary, while the pressure distribution around the cylinder, calculated on the basis of this contour, is shown in figure 7 together with three sets of experimental data from Grove *et al.* (1964). Also shown

† For a description of this method see also Riegels (1961, p. 76), and Thwaites (1960).

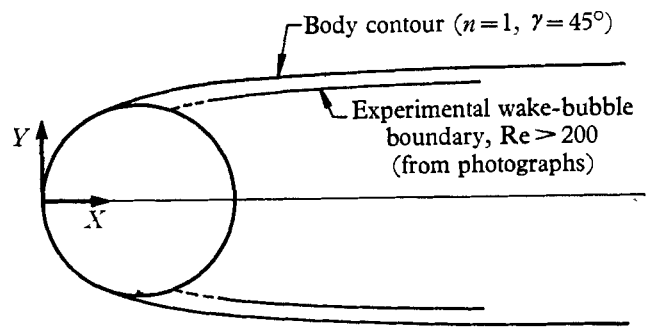

FIGURE 6. Comparison of the body contour with the wake-bubble boundary.

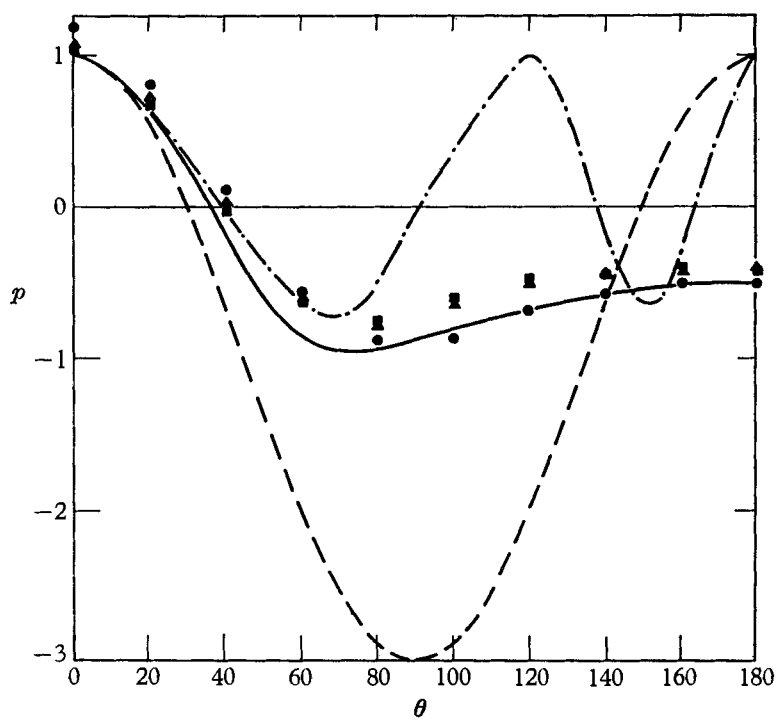

FIGURE 7. Comparison of experimental and calculated pressure distributions. Experimental measurements: ●, Re = 40; ▲, Re = 129; ■, Re = 177. ——, present model; – – –, symmetrical-potential-flow model; — · —, Föppl's vortex model, k = 2·5.

in figure 7 are the pressure profiles from two other inviscid models: the continuous potential flow model, and Föppl's vortex model with its adjustable parameter k set equal to 2·5 (Shair 1963). Clearly, the agreement between the calculations based on the present model and the experimental results is quite satisfactory. Moreover, as shown in Appendix 2, the calculated pressure profiles are indeed insensitive to the assumed shape of the body contour, so that the proposed method appears to be not only exceedingly simple to use but also, from the practical point of view, quite valuable.

Finally, we wish to emphasize once more that, in common with all existing inviscid analyses, the method just described contains certain basic inconsistencies with respect to the experimental observations. For one thing, if one sets $Y'(X) = 0$ for $X > O(1)$ in equation (12), one obtains a pressure recovery along the wake-bubble boundary at a distance $O(1)$ from the centre of the cylinder, which is clearly incompatible with the notion of a stagnant 'inner' wake relative to the external stream. Thus, it is important to realize that this method represents nothing more than an empirical, but apparently successful, technique for calculating approximately the pressure distribution around solid objects in *steady* separated flows.

(*b*) *The location of the point of detachment*

As mentioned earlier, the scheme which was proposed in the preceding section for determining the pressure profile on a bluff object requires that the approximate shape of the wake bubble be known *a priori*. In turn, one of the most important factors that determines this shape is the location of the point of detachment, that is, the point at which the outer flow detaches itself from the surface of the body. Thus, it would be helpful for our scheme if this point could be located theoretically starting from basic principles.

Squire (1934) appears to have been the first to propose that the point of detachment should be identical to the point of separation of the boundary layer, which occurs by definition at the point of zero wall shear stress. Since the latter can be calculated readily via a standard laminar-boundary-layer analysis using the pressure profile that is impressed on the boundary layer by the external flow, one can readily visualize the following iterative procedure. A likely separation point is first selected, following which the pressure profile is determined by means of a suitable inviscid technique. In turn, this is followed by a boundary-layer calculation, resulting in a new separation point, and so on. This scheme forms the basis of Woods' model (see Woods 1961, p. 428) and has also been tried many times before.

Yet, although it is generally assumed that the points of detachment and boundary-layer separation do coincide, or very nearly so, no convincing proof for this assumption appears to have been advanced so far. It is of interest, therefore, to report that, when boundary-layer calculations were performed using the *experimentally measured* pressure profile at $\mathrm{Re} = 177$ together with Stratford's approximate technique as refined by Curl (1960), the shear stress at the wall was found to be positive everywhere along the wetted portion of the perimeter. It is realized of course that this result may not be very meaningful since boundary-layer separation is so dependent on the *slope* of the pressure profile, which, owing to experimental inaccuracies of our pressure measurements, could only be obtained approximately. Nevertheless, this result is reported here in the hope that it may lead to a re-examination of the important phenomenon of 'separation', and of the exact relationship, if any, between the points of boundary-layer separation and detachment of the external flow from the solid surface of a bluff body.

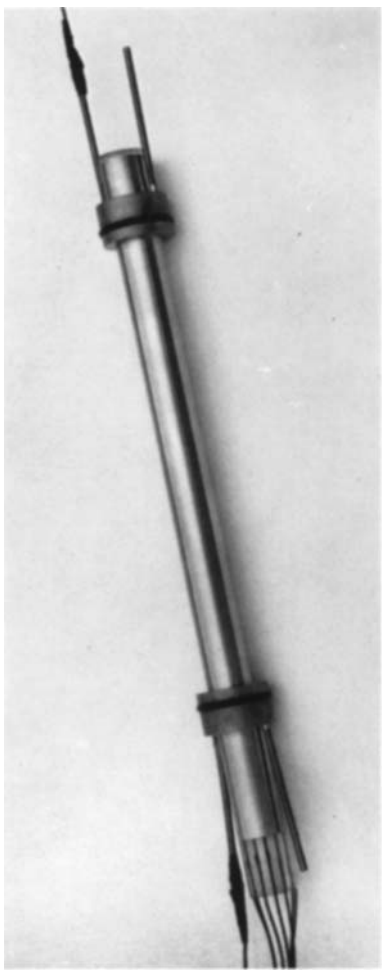

FIGURE 9. The heat-transfer cylinder and core assembly.

(c) *Some estimates regarding the wake-bubble length*

An interesting way of considering the wake bubble can be developed on the basis of the fact that it is in static equilibrium, so that the sum of the forces acting on it in any direction must be zero. As indicated in figure 8, however, the forces acting on the wake bubble are of two types: viscous and pressure forces. Therefore,

$$\int_a p'\mathbf{n}.\mathbf{e}_x ds' + \int_b p'\mathbf{n}.\mathbf{e}_x ds' + F'_v = 0, \tag{13}$$

where a denotes the portion of the wake-bubble boundary in contact with the cylinder, and b denotes the rest of its boundary; p' is the physical pressure, $\mathbf{n}$ the inner unit normal, and $\mathbf{e}_x$ the unit vector in the positive x direction. F'_v is the integral of the viscous forces acting in the positive x direction.

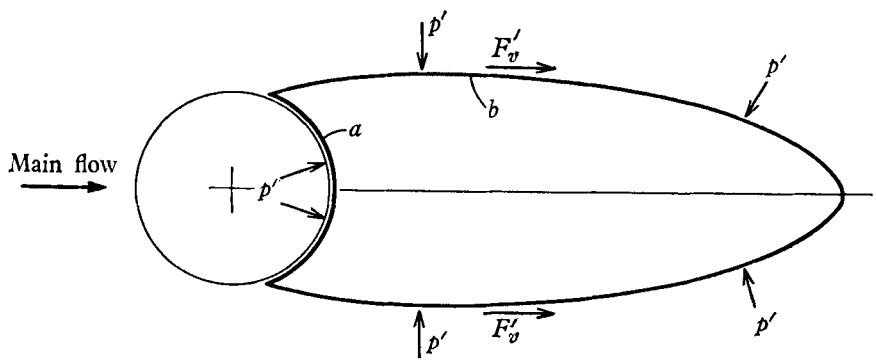

FIGURE 8. The forces acting on the wake bubble.

Equation (13) can be rewritten in the non-dimensional form:

$$\int_a p\mathbf{n}.\mathbf{e}_x ds + \int_b p\mathbf{n}.\mathbf{e}_x ds + \frac{F'_v}{\frac{1}{2}\rho U^2 d} = 0. \tag{14}$$

Now, according to the experimental observations, the pressure coefficient at the rear of the cylinder is approximately $-0{\cdot}45$ at large Reynolds numbers, from which it follows that the value of the first integral, $-A$, will also be approximately $-0{\cdot}45$. On the other hand, the contribution of the second integral will be relatively minor, since $\mathbf{n}.\mathbf{e}_x \sim 0$ everywhere along b except near the tip of the wake bubble where $p \sim 0$. Consequently,

$$F'_v/\tfrac{1}{2}\rho U^2 d = A \cong 0{\cdot}45. \tag{15}$$

Next, since the streamline separating the wake bubble from the main flow is essentially parallel to the x-axis over most if its length, we can set

$$F'_v \cong 2\mu \int_0^{x'_L} \left.\frac{\partial u'}{\partial y'}\right|_{y'^*} dx', \tag{16}$$

where u', x', y' are the physical quantities, y'^* denotes the location of the wake-bubble boundary, and x'_L denotes the length of the wake bubble. As described earlier, however, one of the features of the asymptotic flow is the existence of a viscous shear layer separating the relatively stagnant wake bubble from the

outer flow. Therefore, if we assume for simplicity that the shear layer remains thin along the whole of the wake-bubble boundary, we can determine F'_v approximately by means of a standard boundary-layer analysis with x'_L as the characteristic length. It follows that

$$F'_v \cong C\mu U\,(Ux'_L/\nu)^{\frac{1}{2}}, \tag{17}$$

where C is a constant of proportionality, so that, in view of equation (15),

$$\frac{x'_L}{d} \cong \left(\frac{A}{2C}\right)^2 \mathrm{Re}. \tag{18}$$

Using an entirely different approach then, we have again established, as in § 2, that the wake length is proportional to the Reynolds number, but with the added advantage that equation (18) allows us to arrive at a rough estimate for the constant of proportionality. Thus, by setting $C \cong 0{\cdot}8$, the value obtained by Potter (1957) for the boundary-layer flow of an unbounded fluid stream over another fluid region at rest, and $A \sim 0{\cdot}45$, one obtains

$$\left(\frac{A}{2C}\right)^2 = O(10^{-1}).$$

The experimentally observed values are 0·025 for $d/h = 0{\cdot}2$ and 0·04 for $d/h = 0{\cdot}1$, (see Grove *et al.* 1964), while Taneda's (1956) measurements indicate a value of 0·067 for $d/h < 0{\cdot}03$. The theoretical estimate is therefore in good qualitative agreement with the experimental results.

This work was supported in part by a grant from the Petroleum Research Fund administered by the American Chemical Society, and by a Texaco Corporation fellowship which was awarded to D. D. Snowden. The authors are grateful to these donors for their financial support, and to Dr G. K. Batchelor for his constructive criticism of an earlier version of this paper.

Appendix 1

(*a*) *Experimental equipment and procedure*

All of the heat-transfer experiments were conducted in a tunnel (described in detail by Shah, Petersen & Acrivos 1962) in which a Newtonian lubricating oil with a viscosity of approximately 1 poise was recirculated past a horizontal circular cylinder, which was heated at a constant flux and placed in the test section with its axis normal to the direction of the main flow.†

The cylinder was constructed of thin walled nichrome tubing with a uniform wall thickness of 0·010 in. and an outside diameter of 0·82 in. High current from a regulated a.c. power source was supplied to the cylinder by means of heavy brass rings shrink-fitted onto its ends, and generated a constant and uniform heat flux in the thin cylinder wall. The circumferential surface-temperature distribution at the middle of the cylinder was measured by means of seven copper-constantan thermocouples, located 30° apart, which were positioned in

† Details concerning the method used to obtain velocities in the tunnel test section and a discussion of the effect of confining walls on the velocity profiles and the pressure are given by Grove (1963).

grooves in a cylindrical Lucite core. This core, when fitted inside the cylinder, was surrounded by an air film which served to insulate thermally the inner cylinder surface. Figure 9 (plate 1) illustrates the cylinder and core assembly. A vacuum-tube voltmeter was used to measure the voltage drop between the two brass rings on the cylinder, and, together with the known resistance and cylinder surface area, led to an easy calculation of the heat flux.

(*b*) *Temperature dependent viscosity*

A problem which generally arises in processing experimental heat-transfer data is that the fluid properties are temperature dependent within the thermal boundary layer. Fortunately, however, with the oil used in our experiments, only the variation of the viscosity with temperature had to be taken into account.

First of all, it has been shown (Acrivos 1960) that, for high-Prandtl-number fluids, the Reynolds number upon which the heat transfer depends should be based on the bulk fluid viscosity. In addition, for the case of forced-convection heat transfer at high Prandtl numbers from an isothermal surface to fluids with temperature-dependent viscosity, one can show (Acrivos 1960) that the local Nusselt number is given by

$$\mathrm{Nu} = -\left(\frac{d\theta}{d\eta}\right)_{\eta=0} (\mathrm{Re})^{\frac{1}{2}} \left(\frac{\mathrm{Pr}}{9}\right)^{\frac{1}{3}} \beta^{\frac{1}{2}} \left(\int_{x^*}^{x} \beta^{\frac{1}{2}}\, dx\right)^{-\frac{1}{3}}, \tag{19}$$

where $\beta(x)$ represents the dimensionless velocity gradient at the wall, Pr is based on the viscosity at the temperature of the heated surface, and $(d\theta/d\eta)_{\eta=0}$ is to be obtained from the solution of the energy equation

$$\frac{d^2\theta}{d\eta^2} + 6\frac{d\theta}{d\eta}\left[\int_0^{\eta}\int_0^{z_1} \mu^{-1} dz_2\, dz_1\right] = 0, \tag{20}$$

with the usual boundary conditions, $\theta(0) = 1$ and $\theta(\infty) = 0$, μ being the dimensional viscosity divided by its value at the surface where $\theta = 1$.

Now, when the appropriate expression for the viscosity of our oil as a function of the temperature was inserted into equation (20), the solution was found to be very nearly the same as that for the constant property case. In particular, one can show that in our case

$$-\left(\frac{d\theta}{d\eta}\right)_{\eta=0} \cong \left[\Gamma(\tfrac{4}{3}) + \frac{b}{12}\frac{\Gamma(\frac{5}{3})}{\Gamma(\frac{4}{3})}\right]^{-1}, \tag{21}$$

with b defined as $b \equiv 1 - \mu'_s/\mu'_\infty$, where μ'_s and μ'_∞ are the dimensional viscosities evaluated at the temperature of the heated surface and the bulk fluid, respectively. Of course, with $b = 0$, equation (19) reduces to the constant property solution first developed by Lighthill (1950).

Thus, we see that experimental values of $\mathrm{Nu}/\mathrm{Pr}^{\frac{1}{3}}$ may be computed by basing Pr on the surface viscosity, provided they are multiplied by a suitable correction factor $C \cong 1 - b\Gamma(\frac{5}{3})/12[\Gamma(\frac{4}{3})]^2$, which, for the conditions of our experiments, was always within the range of 0·96 to 1·00.

(c) *Influence of the splitter plate*

Since the presence of a splitter plate in the wake bubble is required in order to maintain a steady separated flow at high Reynolds numbers,† we felt it desirable to check experimentally the influence, if any, of the plate position on the local Nusselt number at the rear of the heated cylinder. Figure 10 shows the variation with c/d of the limiting value of $\mathrm{Nu/Pr^{\frac{1}{3}}}$ at the rear stagnation point of the cylinder. (c is the distance from the centre of the cylinder to the front edge of the splitter plate, and d is the cylinder diameter.) The most important conclusion which one

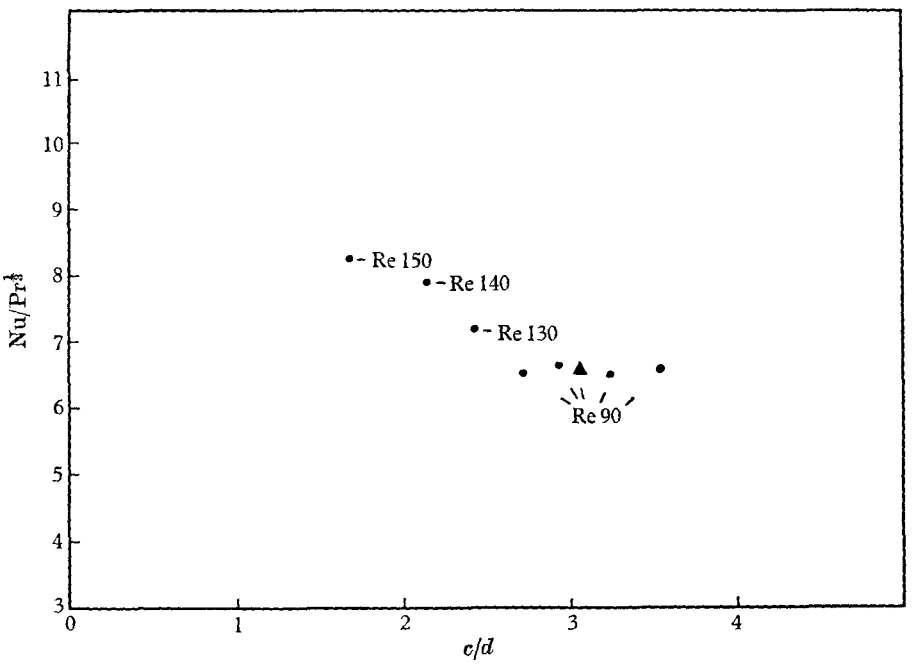

FIGURE 10. The effect of the splitter-plate position on the limiting value of $\mathrm{Nu/Pr^{\frac{1}{3}}}$ at the rear stagnation point. ●, 4 in. splitter plate; ▲, 2 in. splitter plate.

can draw from figure 10 is that if the splitter plate is positioned 'far enough' ($c/d > 2{\cdot}6$) back from the cylinder, its position has no influence on the local Nusselt number. However, at positions nearer to the cylinder than this 'critical' location, both the limiting value of $\mathrm{Nu/Pr^{\frac{1}{3}}}$ and the Reynolds number at which it is reached are increased. (This Reynolds number is shown adjacent to each point in figure 10.) Consequently, all of the experiments reported earlier in this paper were conducted with the plate positioned at a c/d greater than this 'critical' value.

Previous studies, reported by Grove *et al.* (1964), have shown that the size of the splitter plate used to stabilize the wake bubble has no discernible influence on the value of the pressure coefficient at the rear stagnation point of the cylinder, and does not affect the linear relationship between the wake-bubble length and

† Details concerning the use of a splitter plate to stabilize the wake bubble at high Reynolds numbers and on its mounting in the tunnel test section are given in Grove *et al.* (1964).

the Reynolds number. It is therefore not surprising that no influence of the splitter-plate size on the limiting value of $\mathrm{Nu}/\mathrm{Pr}^{\frac{1}{3}}$ at the rear stagnation point of the cylinder was observed with the plate positioned at $c/d > 2{\cdot}6$ (see figure 10).

(*d*) *Influence of natural convection*

An analysis of the variation with Re of local values of $\mathrm{Nu}/\mathrm{Pr}^{\frac{1}{3}}$ at the rear stagnation point of the cylinder showed that, at high Reynolds numbers, the limiting value obtained for $\mathrm{Nu}/\mathrm{Pr}^{\frac{1}{3}}$ was essentially independent of the heat flux that was chosen for the experiment. However, a slight increase in $\mathrm{Nu}/\mathrm{Pr}^{\frac{1}{3}}$ with flux could be detected at lower Reynolds numbers. One may conclude that this influence is probably due to natural convection, since experiments conducted with no flow past the heated cylinder yielded values of the local Nusselt number at the rear stagnation point of the cylinder of approximately 14, or $\mathrm{Nu}/\mathrm{Pr}^{\frac{1}{3}} = 1{\cdot}3\,(\mathrm{Pr} = 1200)$. In contrast, the data at the front stagnation point of the cylinder showed no such influence of the heat flux.

Appendix 2. The approximate pressure calculations

The method, described in § 3, for computing approximately the pressure profile on the cylinder requires the use of a body contour which joins 'smoothly' the cylinder surface and the wake-bubble boundary. Thus, the body should not have any breaks in its contour since the flow of an inviscid fluid around a sharp corner results in either a stagnation point or in an infinite velocity. Furthermore, the curvature of the contour must be continuous or else an infinite pressure gradient will result at the point of discontinuity (Riegels 1961, p. 70). This contour could be chosen in a number of ways. The purpose of this Appendix is to indicate the calculational procedure which was employed and to present some of the pressure profiles which resulted from the various contours that were selected.

A typical contour is shown in figure 11, which also serves to illustrate the notation used. The contour is represented by the function $Y(X)$, where X is the distance from the front stagnation point of the cylinder. Both distances are in terms of the cylinder radius. The contour is divided into two parts,

$$\left.\begin{aligned} Y &= Y_1 \quad \text{for} \quad X < X_s, \\ Y &= Y_2 \quad \text{for} \quad X > X_s, \end{aligned}\right\} \tag{22}$$

where the front part, Y_1, is formed by the cylinder surface, so that

$$Y_1 = [1-(X-1)^2]^{\frac{1}{2}}. \tag{23}$$

The function Y_1 is joined smoothly to the rest of the contour Y_2 at the point X_s by requiring that, as explained above,

$$\left.\begin{aligned} Y_1 &= Y_2 \\ Y_1' &= Y_2' \\ Y_1'' &= Y_2'' \end{aligned}\right\} \quad \text{at} \quad X = X_s, \tag{24}$$

where the primes denote differentiation. The point X_s is related to the joining angle γ by $X_s = 1-\sin\gamma$. (It should be emphasized that the joining angle γ is

not the angle of separation. It is merely a parameter which is adjusted in such a way that the body contour corresponds most closely to the experimentally observed wake-bubble boundary.) The various contours were distinguished by different choices of the function Y_2 as well as by different values of γ.

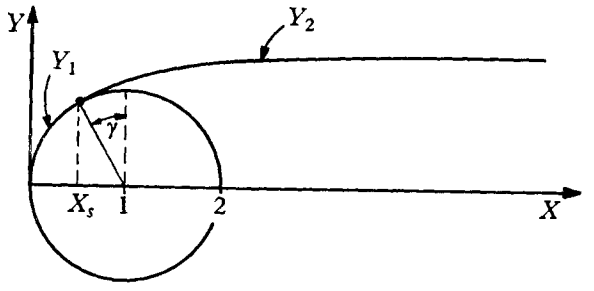

FIGURE 11. The body contour.

In establishing the contours, we were guided by the experimentally observed shape of the wake-bubble boundary, but, since this still left a considerable amount of latitude, it was important to establish how much the pressure distribution around the cylinder was affected by small changes in the assumed contour.

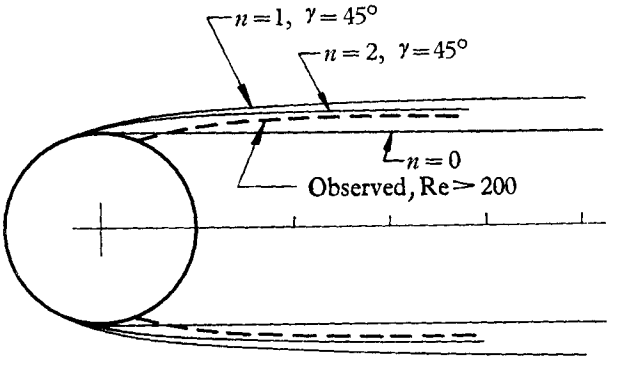

FIGURE 12. Comparison of various open body contours with the photographically observed wake-bubble boundary.

The general formula which was adopted was

$$Y_2 = W - A(X+B)^{-n}. \tag{25}$$

For the case $n = 0$, $Y_2 = \text{const}$. Only the first two matching conditions in equations (24) can then be met and the value of γ was set at 90°. Such a profile, shown in figure 12, has been studied by Riegels (1948, 1961), and the pressure distribution around the cylinder as obtained from his results is shown in figure 13. (As mentioned in § 3, the pressure at any point on the cylinder surface was taken to be the same as the pressure on the contour at the corresponding value of X.)

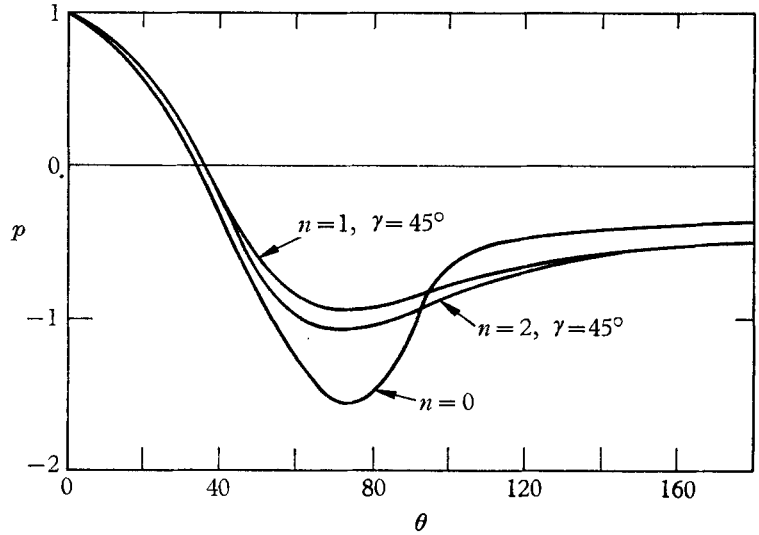

FIGURE 13. The pressure distribution around the cylinder based on various open body contours.

For the cases $n = 1$ and $n = 2$, the values of the constants W, A and B were determined from the matching conditions, equations (24), for a given choice of n and γ (or X_s). Once Y_2 was thus defined, the velocity distribution was calculated using equation (12). The evaluation of the integral is somewhat laborious but leads to simple closed form expressions which are presented elsewhere (Grove 1963).

The contours with $\gamma = 45°$ are shown in figure 12 for both $n = 1$ and $n = 2$. It can be seen that both these contours correspond closely to the experimentally observed wake bubble boundary.

Contours and pressure distributions were computed for different values of γ ranging between 10° and 60°. It was found that the pressure distributions were influenced only slightly by the choice of γ, and that all the calculated pressure profiles were located between the profile for $n = 0$ and the profile for $n = 1$, $\gamma = 45°$, both of which are shown in figure 13. 'Reasonable' contours which closed at various distances downstream of the cylinder were also studied, and the resulting pressure distributions were again found to be similar to the ones shown on figure 13 (Grove 1963).

On the basis of a comparative study of these contours, both open and closed, one can then conclude that (i) the pressure distribution around the cylinder is quite insensitive to the shape of the assumed body contour, and (ii) the more closely the assumed contour conforms to the experimentally observed wake-bubble boundary, the more closely the calculated pressure distribution agrees with the experiments.

REFERENCES

ACRIVOS, A. 1960 Solution of the laminar boundary layer energy equation at high Prandtl numbers. *Phys. Fluids*, **3**, 657.

BATCHELOR, G. K. 1956 A proposal concerning laminar wakes behind bluff bodies at large Reynolds number. *J. Fluid Mech.* **1**, 388.

CURL, N. 1960 The estimation of laminar skin friction, including the effects of distributed suction. *Aero. Quart.* **11**, 1.

GROVE, A. S. 1963 Ph.D. thesis, University of California, Berkeley.

GROVE, A. S., SHAIR, F. H., PETERSEN, E. E. & ACRIVOS, ANDREAS 1964 An experimental investigation of the steady separated flow past a circular cylinder. *J. Fluid Mech.* **19**, 60.

LIGHTHILL, M. J. 1950 Contributions to the theory of heat transfer through a laminar boundary layer. *Proc. Roy. Soc.* A, **202**, 369.

MORGAN, G. W. & WARNER, W. H. 1956 On heat transfer in laminar boundary layers at high Prandtl number. *J. Aero. Sci.* **23**, 937.

POTTER, O. E. 1957 Laminar boundary layers at the interface of co-current parallel streams. *Quart. J. Mech. Appl. Math.* **10**, 302.

PROUDMAN, I. 1960 An example of steady laminar flow at large Reynolds number. *J. Fluid Mech.* **9**, 593.

RIABOUCHINSKY, D. 1920 On the steady flow motions with free surfaces. *Proc. Lond. Math. Soc.* **19**, 206.

RIEGELS, F. W. 1948 Das Umströmungsproblem bei inkompressiblen Potentialströmungen. *Ingenieur-Archiv.* **16**, 373.

RIEGELS, F. W. 1961 *Aerofoil Sections.* London: Butterworths.

ROSHKO, A. 1954 A new hodograph for free-streamline theory. *NACA TN* 3168.

SHAH, M. J., PETERSEN, E. E. & ACRIVOS, A. 1962 Heat transfer from a cylinder to a power-law non-Newtonian fluid. *A.I.Ch.E. J.* **8**, 542.

SHAIR, F. H. 1963 Ph.D. thesis, University of California, Berkeley.

SQUIRE, H. B. 1934 On the laminar flow of a viscous fluid with vanishing viscosity. *Phil. Mag.* **7**, 1150.

TANEDA, S. 1956 Experimental investigation of the wakes behind cylinders and plates at low Reynolds numbers. *J. Phys. Soc. Japan*, **11**, 302.

THWAITES, B. (Ed.) 1960 *Incompressible Aerodynamics*, p. 131. Oxford: Clarendon Press.

WOODS, L. C. 1955 Two-dimensional flow of a compressible fluid past given curved obstacles with wakes. *Proc. Roy. Soc.* A, **227**, 367.

WOODS, L. C. 1961 *The Theory of Subsonic Plane Flow.* Cambridge University Press.

WU, T. Y. 1962 A wake model for free-streamline flow theory. *J. Fluid Mech.* **13**, 161.